3. Miyayama S, Matsui O, Akakura Y et al (2001) Hepatocellular carcinoma with blood supply from omental branches: treatment with transcatheter arterial embolization. J Vasc Interv Radiol 12:1285–1290
4. Chung JW, Park JH, Han JK et al (1998) Transcatheter oily chemoembolization of the inferior phrenic artery in hepatocellular carcinoma: the safety and potential therapeutic role. J Vasc Interv Radiol 9:495–500
5. Kim HC, Chung JW, Lee W et al (2005) Recognizing extrahepatic collateral vessels that supply hepatocellular carcinoma to avoid complications of transcatheter arterial chemoembolization. Radiographics 25(suppl):S25–S39
6. Miyayama S, Matsui O, Taki K et al (2006) Extrahepatic blood supply to hepatocellular carcinoma: angiographic demonstration and transcatheter arterial chemoembolization. Cardiovasc Intervent Radiol 29:39–48
7. Miyayama S, Matsui O, Nishida H et al (2003) Transcatheter arterial chemoembolization for unresectable hepatocellular carcinoma fed by the cystic artery. J Vasc Interv Radiol 14:1155–1161
8. Nakai M, Sato M, Kawai N et al (2001) Hepatocellular carcinoma: involvement of the internal mammary artery. Radiology 219:147–152
9. Park SI, Lee DY, Won JY et al (2003) Extrahepatic collateral supply of hepatocellular carcinoma by the intercostal arteries. J Vasc Interv Radiol 14:461–468
10. Kodama Y, Shimizu T, Endo H et al (2002) Spontaneous rupture of hepatocellular carcinoma supplied by the right renal capsular artery treated by transcatheter arterial embolization. Cardiovasc Intervent Radiol 25:137–140
11. Suh SH, Won JY, Lee DY et al (2005) Chemoembolization of the left inferior phrenic artery in patients with hepatocellular carcinoma: radiologic findings and clinical outcome. J Vasc Interv Radiol 16:1741–1745
12. Kim HC, Chung JW, Jae HJ et al (2006) Hepatocellular carcinoma: transcatheter arterial chemoembolization of the gonadal artery. J Vasc Interv Radiol 17:703–709
13. Uflacker R (1997) Atlas of vascular anatomy: angiographic approach. Williams & Wilkins, Baltimore, MD, p 418
14. Miyayama S, Matsui O, Taki K et al (2004) Transcatheter arterial chemoembolization for hepatocellular carcinoma fed by the reconstructed inferior phrenic artery: anatomical and technical analysis. J Vasc Interv Radiol 15:815–823
15. Chung JW, Park JH, Han JK et al (1996) Hepatic tumors: predisposing factors for complications of transcatheter oily chemoembolization. Radiology 198:33–40
16. Arora R, Soulen MC, Haskal ZJ (1999) Cutaneous complications of hepatic chemoembolization via extrahepatic collaterals. J Vasc Interv Radiol 10:1351–1356
17. Caglar S, Dolgun H, Ugur HC et al (2004) Extraforaminal lumbar arterial anatomoy. Surg Neurol 61:29–33
18. Miyayama S, Yamashiro M, Okuda M, et al. (2008) Anastomosis between the hepatic artery and the extrahepatic collateral or between extrahepatic collaterals: observation on angiography. J Med Imaging Radiat Oncol (in press)

Hepatology Research 2009; 39: 374–381 doi: 10.1111/j.1872-034X.2008.00465.x

Original Article

Histopathological findings after ultraselective transcatheter arterial chemoembolization for hepatocellular carcinoma

Shiro Miyayama[1], Takeshi Mitsui[2], Yoh Zen[3], Yoshiko Sudo[4], Masashi Yamashiro[1], Miho Okuda[1], Yuichi Yoshie[1], Taku Sanada[5], Kazuo Notsumata[5], Nobuyoshi Tanaka[5] and Osamu Matsui[6]

[1]*Departments of Diagnostic Radiology,* [2]*Surgery,* [5]*Internal Medicine, and* [4]*Pathology, Fukuiken Saiseikai Hospital, Fukui, and* [6]*Departments of Radiology and* [3]*Pathology, Kanazawa University Graduate School of Medical Science, Kanazawa, Japan*

Aim: To evaluate the histopathologic findings in the surgical specimen of hepatocelluar carcinoma after transcatheter arterial chemoembolization (TACE) at the most distal portion of the sub-subsegmental artery of the liver (ultraselective TACE).

Methods: Histolopathologic findings from nine tumors with a mean diameter of 3.1 cm ± 1.7 from patients who underwent hepatectomy after ultraselective TACE were evaluated, especially with regard to the relationship between peritumoral liver parenchymal necrosis and portal vein visualization during TACE. Portal vein visualization was classified into three grades by a spot digital radiograph obtained just after TACE: 0, no obvious portal vein visualization; 1, visualization of the portal vein adjacent to the tumor; and 2, visualization in the whole embolized area or extending into the surrounding non-embolized areas. Unenhanced computed tomography (CT) was obtained 1 week later and surgical resection was performed 37 ± 6.3 days after ultraselective TACE.

Results: Portal vein visualization during TACE was classed as grade 1 in 5 tumors and grade 2 in 4. Histopathologically, complete tumor necrosis was observed in 7 tumors (77.8%). In 2 tumors (1 of grade 1, the other grade 2), a small viable portion or viable daughter nodule was seen. Macroscopic parenchymal necrosis adjacent to the tumor was observed in all 4 grade 2 tumors including gas-containing areas on CT obtained 1 week after TACE.

Conclusions: Ultraselective TACE induces not only complete tumor necrosis but also peritumoral parenchymal necrosis, similar to that after radiofrequency ablation, when the portal veins are markedly visualized during the TACE procedure.

Key words: hepatocellular carcinoma, histopathologic study, peritumoral parenchymal necrosis, transcatheter arterial chemoembolization

INTRODUCTION

HEPATOCELLULAR CARCINOMA (HCC) is one of the most common malignant tumors in East Asia. The prognosis of patients with inoperable HCC has improved with advances in therapeutic options such as local ablation therapies in addition to transcatheter arterial chemoembolization (TACE).[1–11]

In our previous report,[8] local recurrence rates of tumors showing marked portal vein visualization during ultraselective TACE (TACE at the most distal portion of the sub-subsegmental artery of the liver) were significantly lower than those of tumors with slight or no portal vein visualization. This suggests that the blockage of both arterial and portal blood flow may have been achieved when portal veins are markedly apparent during TACE.[3,5,7,8]

In the present study, we evaluated histopathologic findings of surgical specimens after ultraselective TACE, with special regard to the relationship between peritumoral parenchymal necrosis and portal vein visualization during the TACE procedure.

Correspondence: Dr Shiro Miyayama, Department of Diagnostic Radiology, Fukuiken Saiseikai Hospital, 7-1, Funabashi, Wadanaka-cho, Fukui 918-8503, Japan. Email: s-miyayama@fukui.saiseikai.or.jp

Received 13 August 2008; Revised 26 September 2008; Accepted 28 September 2008.

MATERIALS AND METHODS

WE RETROSPECTIVELY ANALYZED histopathologic findings in patients who underwent surgical hepatic resection after ultraselective TACE. Institutional

review board approval is not required at our institution for this type of study. Written informed consent was obtained from each patient before the TACE procedure and hepatectomy.

Between January 2002 and September 2007, 9 patients with HCC underwent surgical hepatic resection after ultraselective TACE. Tables 1 and 2 shows patient characteristics. There were 5 men and 4 women and the mean patient age was 57.9 years ± 5.8. All patients had chronic hepatitis or liver cirrhosis. This was related to hepatitis C virus in 3 patients, hepatitis B virus in 3 patients, to both hepatitis B and C in 1 patient and the etiology was unknown in 2 patients. All patients had a single HCC lesion with a mean tumor diameter 3.1 cm ± 1.7 (range 1.0–6.5 cm). A combined therapy of TACE and radiofrequency (RF) ablation was planned in all patients and TACE was performed sequentially after diagnostic angiography and CT-arteriography, however, surgical resection was finally decided because of tumor size and/or location, hepatic function reserve, or patient's selection.

TACE procedure

After confirmation of the tumor stain on angiography, a 2-F tip (Progreat α; Terumo, Tokyo, Japan) or 2.4-F tip (Microferret; Cook, Bloomington, IN, USA) microcatheter was inserted into the distal portion of the tumor-feeding sub-subsegmental artery through a 4-F catheter placed in the celiac artery, superior mesenteric artery, or common hepatic artery. To navigate the microcatheter, a 0.016-inch guide wire (GT-wire; Terumo) was used in all patients.

After the microcatheter was inserted into the target branch, 0.5 mL of 2% lidocaine (Xylocaine; Fujisawa, Osaka, Japan) was intraarterially injected to prevent pain and vasospasm. First, a mixture of 2–6 mL of iodized oil (Lipiodol; Andre Guerbet, Aulnaysous-Bois, France) (mean, 3.9 mL ± 1.5), 10–30 mg of epirubicin (Farmorbicin; Kyowa Hakko, Tokyo, Japan), and 2–6 mg of mitomycin C (Mitomycin; Kyowa Hakko) was slowly injected through the catheter. The total amount of iodized oil was determined based on the tumor size (almost equal to the diameter of the tumor, e.g., a 3-cm tumor with 3 mL of iodized oil). Second, gelatin sponge (Gelfoam; Upjohn, Kalamazoo, MI) particles that were cut into approximately 0.5-mm cubes, and crushed into less than 0.2-mm particles by pumping using a three-way stopcock valve and two 2.5 mL syringes, were injected to obstruct the tumor-feeding branch completely. Since January 2007, gelatin sponge particles (Gelpart; Nippon Kayaku, Tokyo, Japan) 1 mm

Table 1 Summary of laboratory data in nine patients

Case No./ Age (year)/Sex	Etiology	AST (IU/L)	ALT (IU/L)	Total bilirubin (mg/dL)	Albumin (g/dL)	PLT count (/μL)	HPT (%)	PT-INR	ICGR 15 (%)	AFP (ng/mL)	PIVKA-II (mAU/mL)
1/67/M	HB	44	27	1.3	4.8	15.9	112	0.96	9.0	3	32
2/58/M	Unknown	33	31	0.9	4.2	22.2	79	1.09	3.0	3	97
3/59/M	HB+HCV	31	20	0.3	4.4	12.1	72	1.14	5.5	5	74
4/58/M	Unknown	23	18	0.6	4.6	18.7	150	0.97	5.6	6	20
5/62/M	HB	143	93	0.7	4.1	14.8	100	1.01	9.2	8	1244
6/45/F	HCV	25	32	0.8	4.6	12.8	129	0.94	1.2	7	20
7/59/F	HCV	44	65	0.5	4.3	12.7	115	1.05	6.9	34	42
8/58/F	HCV	56	57	0.8	3.9	8.8	80	1.09	18.4	6	13
9/55/F	HB	18	15	0.6	4.1	11.2	111	1.08	1.8	2226	95

AFP, alpha-fetoprotain; AST, asparatate aminotransferase; ALT, alanine aminotransferase; HBV, hepatitis C virus; HCV, hepatitis C virus; HPT, hepaprastin test; ICGR 15, indocyanine green retention at 15 minutes; PIVKA-II, protein induced by vitamin K absence or antagonist-II; PLT, platelet; PT-INR, prothrombin time-international normalized ratio.

Table 2 Summary of data in 9 patients who underwent hepatectomy after ultraselective transcatheter arterial chemoembolization

Case No./ Age (year)/ Sex	Tumor location*	Size (cm)	Visualization of portal vein (Grade)	Pathologic findings	Operation procedure	Massive peritumoral necrosis
1/67/M	S8	4.2	1	S8 subsegmentectomy	Viable portion in the capsule (2 mm in diameter) Viable daughter nodule (4 mm in diameter)	None
2/58/M	S8-5	4.5	1	Anterior segmentectomy	Complete necrosis	None
3/59/M	S8	2.5	1	S8 subsegmentectomy	Complete necrosis	None
4/58/M	S5	2.3	1	S5 subsegmentectomy	Complete necrosis	None
5/62/M	S8	6.5	1	S8 subsegmentectomy	Complete necrosis	None
6/45/F	S3	1	2	Lateral segmentectomy	Complete necrosis	(+)
7/59/F	S5	1.3	2	S5 subsegmentectomy	Complete necrosis	(+)
8/58/F	S7	2.8	2	S7 subsegmentectomy	Viable portion at the periphery (4 mm in diameter)	(+)
9/55/F	S5-6	2.7	2	S5 subsegmentectomy	Complete necrosis	(+)

*Liver segment according to Couinaud's classification.

in diameter were crushed in the same fashion and injected. A spot radiograph was obtained for each tumor just after the TACE procedure in order to evaluate the degree of portal vein visualization. The TACE procedure was terminated when the targeted tumor stain disappeared on angiography. If other feeding branches were demonstrated on angiography, TACE was also performed through these branches. Unenhanced CT was obtained 1 week after TACE to check iodized oil accumulation in the tumor and surrounding liver parenchyma in all patients.

Iodized oil injection was stopped when the portal vein extending to the embolized area appeared. When the flow of the tumor-feeding branch was unexpectedly stopped before adequate portal vein visualization, iodized oil injection was paused and 0.5-μg of prostaglandin E1 (Liple; Mitsubishi Pharma, Osaka, Japan) was administered through the catheter to increase arterial flow. In addition, the microcatheter was advanced more distally to inject embolic materials, if possible, so as to inject these materials with slight force until backflow was observed at the initial injection point. Iodized oil injection was restarted after recovering the flow of the tumor-feeding branch. However, iodized oil injection was ceased when the tumor-feeding branch did not flow despite several efforts.

Classification of portal vein visualization

Portal vein visualization was evaluated by a spot digital radiograph obtained just after TACE. Degrees of portal vein visualization due to overflow of embolic materials were divided into three grades:[8] 0 no visualization, no obvious branching portal vein visualization; 1 slight visualization, visualization of the portal vein adjacent to the tumor; and 2 marked visualization, marked visualization of the portal veins in the whole embolized area or extending into surrounding non-embolized areas (Fig. 1).

Histopathologic examination

Hepatectomy was performed 37 days ± 6.3 (range, 26–48 days) after TACE. The surgical specimens were cut into 5-mm thick after fixation in 10% formalin. Sections were cut along the same axis as the computed tomography (CT) images. Macroscopically, it was determined whether massive peritumoral necrosis was present. All specimens were stained with hematoxylin and eosin and the degree of the main tumor necrosis and residual viable cells were microscopically evaluated.

RESULTS

ALL RESULTS OF each tumor were summarized in Table 2.

Grades of portal vein visualization

Two feeding branches were embolized in six tumors (Figs 2 and 3) and one feeding branch was embolized in three tumors (Fig. 4). Portal vein visualization was classed as grade 1 in five tumors (Fig. 4) and grade 2 in four tumors (Figs 2 and 3). On 1 week after CT, iodized oil was densely accumulated throughout the entire

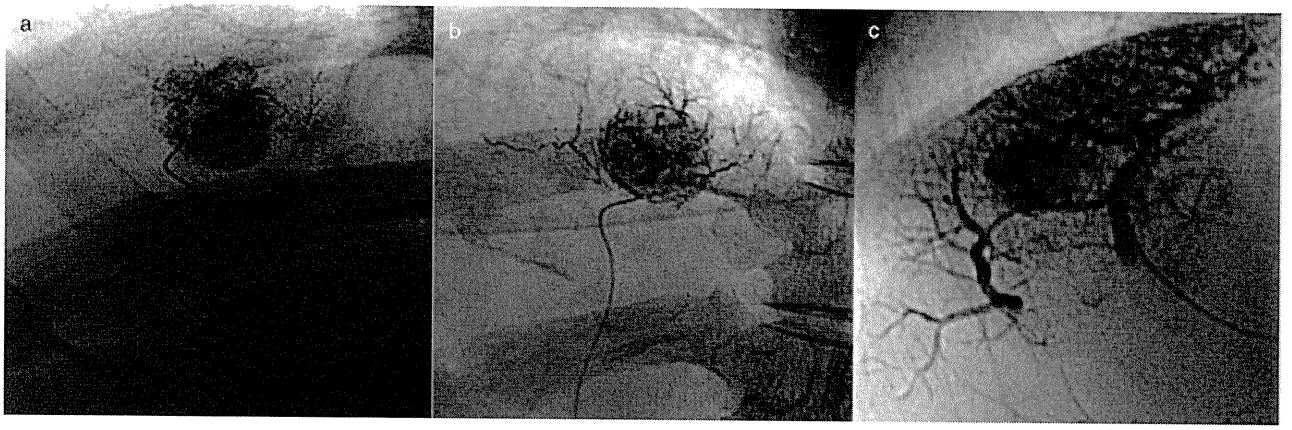

Figure 1 Grades of portal vein visualization. (a) Grade 0, no obvious branching portal vein visualization. (b) Grade 1, visualization of the portal vein adjacent to the tumor. (c) Grade 2, marked visualization of the portal veins in the whole embolized area or extending into the surrounding non-embolized areas.

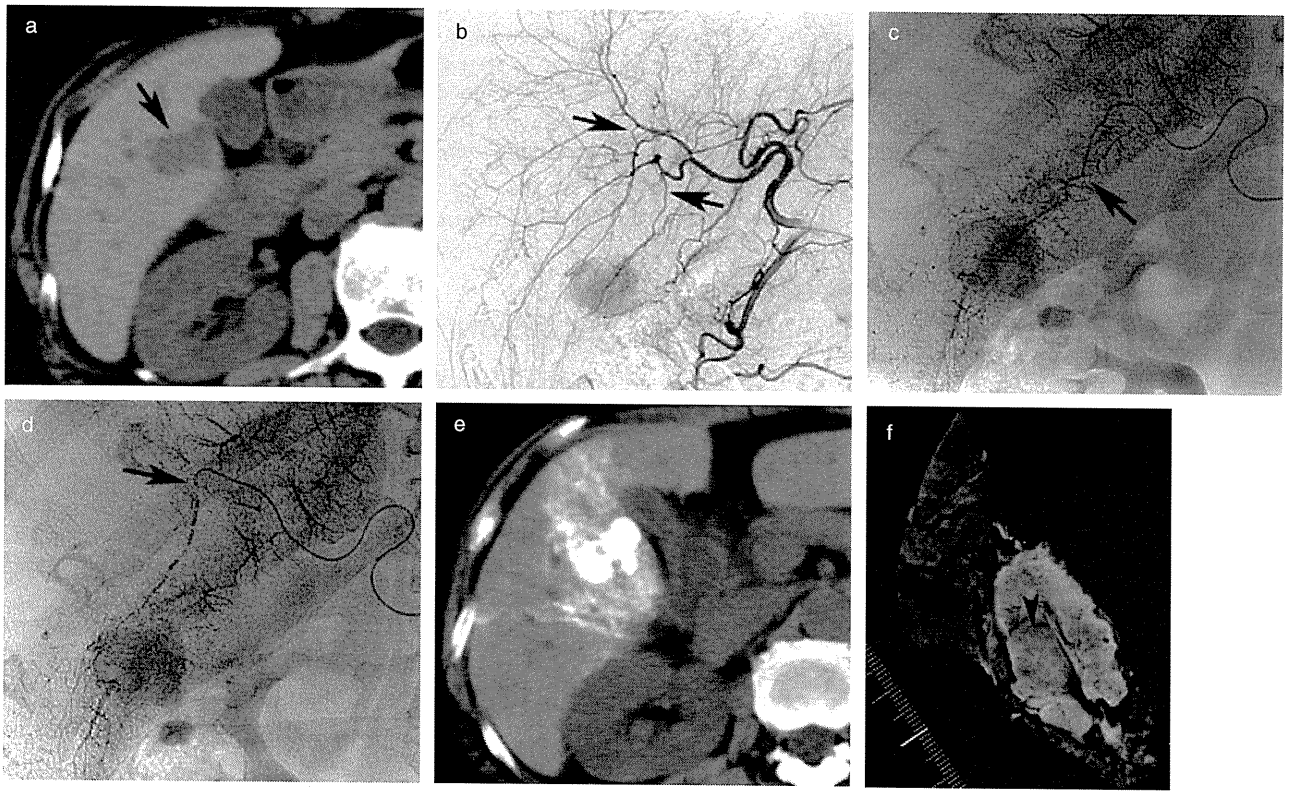

Figure 2 A 55-year-old woman with hepatocellular carcinoma who underwent hepatic resection after ultraselective transcatheter arterial chemoembolization (TACE; Patient 9). (a) Unenhanced computed tomography (CT) shows a hypoattenuationg tumor between the boundary of Segment 5 and 6 (arrow). (b) Common hepatic arteriogram shows a tumor stain supplied by two feeding branches (arrows). (c) First, the tumor-feeding branch of A6 was selected and TACE was performed. The arrow indicates the catheter tip. (d) Second, the tumor-feeding branch of A5 was selected and TACE was performed. Portal veins markedly appeared extending the embolized area during TACE of two branches and classed as grade 2. The arrow indicates the catheter tip. (e) CT obtained 1 week after TACE shows dense iodized oil accumulation in the tumor. (f) In the surgical specimen, complete necrosis of the tumor is seen (arrowhead). Peritumoral necrosis surrounding the tumor (arrow) is also seen.

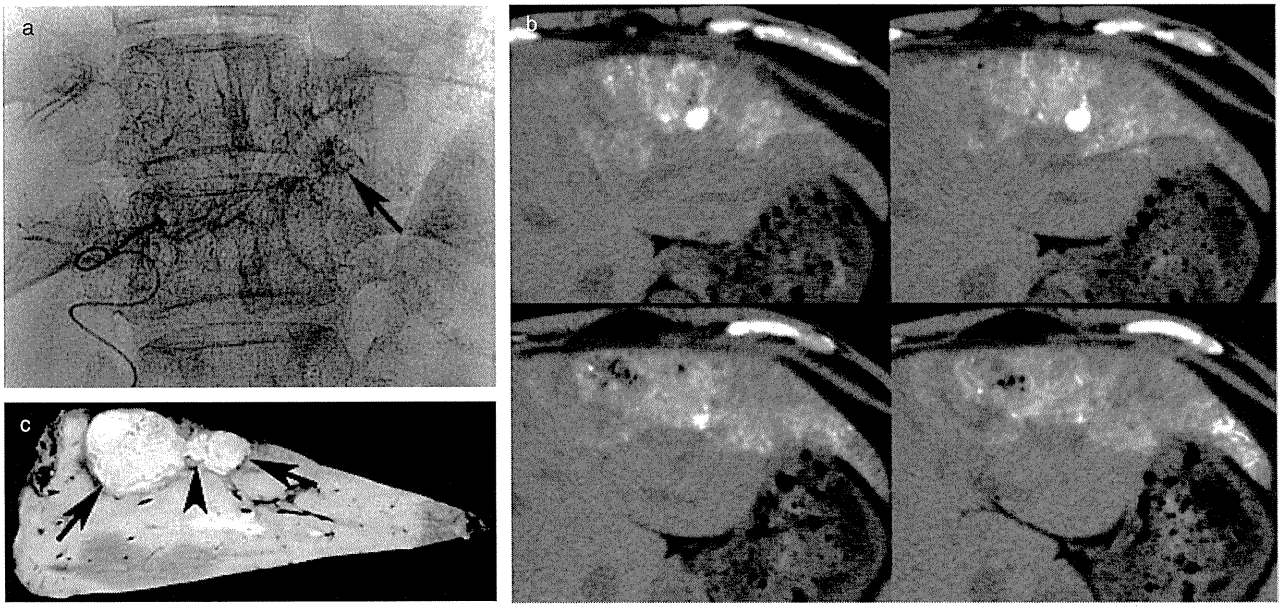

Figure 3 A 45-year-old woman with hepatocellular carcinoma who underwent hepatic resection after ultraselective transcatheter arterial chemoembolization (TACE; Patient 6). (a) Two feeding branches of A3 were embolized and portal vein visualization was classed as grade 2. The arrow indicates the tumor. (b) Computed tomography obtained 1 week after TACE shows dense iodized oil accumulation in the tumor. Gas is also seen in the surrounding liver parenchyma. (c) In the surgical specimen, complete necrosis of the tumor (arrowhead) is seen. Peritumoral necrosis (arrows) adjacent to the tumor is also seen.

tumor in all nine tumors (Figs 2 and 3). In three of four grade 2 tumors, gas in the portal veins was observed in the surrounding liver parenchyma (Fig. 3). Clinical symptoms suggesting abscess formation, such as prolonged high fever, was not observed in any patient.

Histopathologic findings

Complete tumor necrosis was observed in seven of nine tumors (77.8%), four grade 1 tumors and three grade 2 tumors (Figs 2 and 3). In one grade 1 tumor measuring 4.2 cm in diameter, a small viable tumor focus measuring 2 mm in diameter was found within the tumor pseudocapsule. In addition, a viable daughter nodule measuring 4 mm in diameter was observed near the tumor (Fig. 4). In the remaining grade 2 tumor measuring 2.8 cm in diameter protruding to a bare area from the liver surface, a small viable tumor nest measuring 4 mm in diameter was found at the periphery of the tumor. In this case, parasitic blood supply was suspected as the cause of tumor tissue survival.

Macroscopically, peritumoral parenchymal necrosis was found in all four grade 2 tumors (Figs 2 and 3). In three grade 2 tumors with gas in the portal veins on CT obtained 1 week after TACE, the gas-containing area also showed necrosis in the surgical specimen (Fig. 3). Scattered microscopic necrotic foci were found in the embolized area of all grade 1 tumors, but there was no apparent macroscopic parenchymal necrosis.

DISCUSSION

IN PATIENTS WITH inoperable HCC, local control of the tumor may be directly connected to patient prognosis. Among several therapeutic options for HCC, it is generally considered that RF ablation has a stronger therapeutic effect than TACE.[9,10] Lin *et al.* reported that local recurrence rate of HCCs with diameters smaller than 3 cm treated with RF ablation was 10% at 1 year, 14% at 2 years, and 14% at 3 years.[9] Conversely, Kim *et al.* reported that 36% of Edmondson-Steiner grade II HCCs smaller than 3 cm in diameter recurred after RF ablation.[11] However, tumors that are located near vulnerable strictures, such as the main portal vein, inferior vena cava, gallbladder, or alimentary tract, are not generally candidates for RF ablation.[10] Additionally, in the majority of patients with HCC initially treated by some therapeutic options other than TACE, TACE may be required during the subsequent course due to the high incidence of tumor recurrence.[12] Therefore, TACE still plays an important role in the treatment of inoperable HCC and the advancement of TACE technology remains critical.

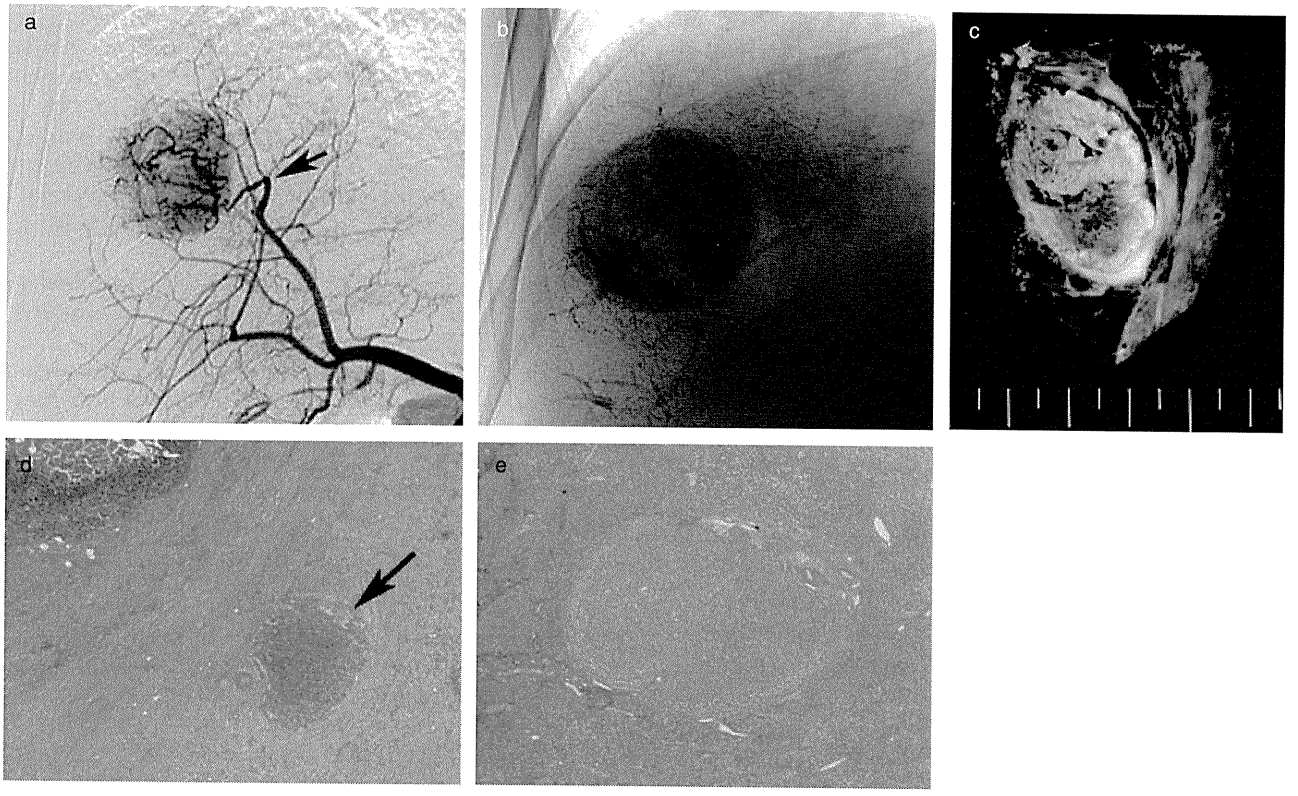

Figure 4 A 67-year-old man with hepatocellular carcinoma who underwent hepatic resection after ultraselective transcatheter arterial chemoembolization (TACE; Patient 1). (a) Common hepatic arteriogram shows a hypervascular tumor. TACE was performed at one branch of A8 (arrow). (b) Spot radiograph obtained immediately after TACE shows that portal veins appears mainly near the tumor (grade 1). (c) In the surgical specimen, massive necrosis of the tumor is seen, however, peritumoral necrosis is not seen. (d) Microscopically, a small viable tumor focus measuring 2 mm in diameter is found within the tumor pseudocapsule (arrow) (hematoxylin and eosin staining, 20 ×). (e) In addition, a viable daughter nodule measuring 4 mm in diameter is observed near the tumor (hematoxylin and eosin staining, 20 ×).

One important cause of tumor tissue survived following TACE is thought to be portal venous supply to tumors appearing when the hepatic artery is embolized. Ekelund *et al.* investigated blood supply in rats with experimental liver tumors after arterial embolization with gelatin sponge powder or ethanol.[13] They found that the portal venous blood supply to tumors clearly increased after arterial embolization. In addition, some of the capsular and/or extracapsular invasion of tumor cells is supplied by both the hepatic artery and portal vein.[14] Well-differentiated tumor portions fed by the portal vein are also present in early-stage HCC.[15,16] These tumor cells may survive after embolization of the hepatic artery alone.

Nakamura *et al.* reported that TACE with a large volume of iodized oil in a limited area of the liver induced not only massive necrosis of the tumor but also atrophy of the surrounding liver parenchyma.[3] Matsuo *et al.* reported that complete necrosis was histologically seen in tumors with dense iodized oil accumulation and portal vein visualization during the TACE procedure.[5] It is also reported that local recurrence rates of tumors with marked portal vein visualization during TACE were significantly lower than those of tumors with slight or no portal vein visualization.[7,8] These reports suggest that iodized oil injected into the feeding artery of HCC flows into the portal vein and can block it. And, as a result, blockage of both arterial and portal blood flow may be achieved. In our experience, hypovascular tumor portions of early-stage HCC also become necrotic with high frequency following ultraselective TACE.[16]

In the present study, massive peritumoral necrosis was seen in all tumors with marked portal vein visualization during the TACE procedure. This suggests that TACE can develop hepatic necrosis similar to that after RF ablation and may also destroy not only the tumor portions sup-

plied by both arterial and portal blood but also the non-tumorous liver parenchyma. Iodized oil injected into the hepatic artery flows into the portal vein through arterioportal communications.[17] In addition, some of the injected iodized oil flows into the portal vein through tumor drainage,[18] where HCC cells spread mainly via the portal system and form intrahepatic satellite lesions.[19] Therefore, blockage of tumor drainage by iodized oil may contribute to the prevention of tumor spread via the portal system or control preexisting microsatellite lesions, and may reduce the incidence of locoregional tumor recurrence after TACE.

This study suggests that ultraselective TACE has therapeutic effects that are strong enough to induce necrosis of non-tumorous liver parenchyma because a relatively large amount of embolic materials is injected with slight force not only into the artery but also into the portal vein. Therefore, the embolized area should be minimumed to reduce the adverse effects and catheterization at the most distal portion is essential. Intraprocedural monitoring of the embolized area using a unified CT-angiography system or cone-beam CT technology should also be performed to facilitate an effective TACE procedure.[6,20] On CT obtained 1 week after TACE, gas in the portal veins was observed and the area became necrotic in the surgical specimen. We speculate that gas in the portal vein in the embolized area may originate from air contaminating the embolic materials during the preparation of gelatin sponge slurry and may not be an indication of abscess formation.

The limitation of our method is that the degree of portal vein visualization can not intentionally be controlled in some tumors.[8] Moreover, it is not certain how long the portal blood flow is affected after TACE. In addition, it has not been histologically confirmed whether gelatin sponge particles pass through arterioportal communications or tumor drainage because these are resolved for a few weeks before performing hepatectomy.

In summary, ultraselective TACE frequently induces not only complete tumor necrosis but also peritumoral parenchymal necrosis when portal veins markedly appear during the TACE procedure. This method may reduce the incidence of locoregional tumor recurrence after TACE.

REFERENCES

1 Yamada R, Sato M, Kawabata M *et al.* Hepatic artery embolization in 120 patients with unresectable hepatoma. *Radiology* 1983; **148**: 397–401.
2 Uchida H, Ohishi H, Matsuo N *et al.* Transcatheter hepatic segmental arterial embolization using Lipiodol mixed with an anticancer drug and Gelfoam particles for hepatocellular carcinoma. *Cardiovasc Intervent Radiol* 1990; **13**: 140–5.
3 Nakamura H, Hashimoto T, Oi H, Sawada S, Furui S, Monzen M. Treatment of hepatocellular carcinoma by segmental hepatic artery injection of adriamycin-in-oil emulsion with overflow to segmental portal tract. *Acta Radiol* 1990; **31**: 347–9.
4 Matsui O, Kadoya M, Yoshikawa J *et al.* Small hepatocellular carcinoma: treatment with subsegmental transcatheter arterial embolization. *Radiology* 1993; **188**: 79–83.
5 Matsuo N, Uchida H, Nishimine K *et al.* Segmental transcatheter hepatic artery chemoembolization with iodized oil for hepatocellular carcinoma: antitumor effect and influence on normal tissue. *J Vasc Interv Radiol* 1993; **4**: 543–9.
6 Takayasu K, Muramatsu Y, Maeda T *et al.* Targeted transarterial oily chemoembolization for small foci of hepatocellular carcinoma using a unified helical CT and angiography system: analysis of factors affecting local recurrence and survival rates. *AJR Am J Roentogenol* 2001; **176**: 681–8.
7 Iwamoto S, Sanefuji H, Okuda K. Angiographic subsegmentectomy for the treatment of patients with small hepatocellular carcinoma. *Cancer* 2003; **97**: 1051–6.
8 Miyayama S, Matsui O, Yamashiro M *et al.* Ultraselective transcatheter arterial chemoembolization with a 2-F tip microcatheter for small hepatocellular carcinomas: relationship between local tumor recurrence and visualization of the portal vein with iodized oil. *J Vasc Interv Radiol* 2007; **18**: 365–76.
9 Lin SM, Lin CJ, Lin CC, Hsu CW, Chen YC. Randomised controlled trial comparing percutaneous radiofrequency thermal ablation, percutaneous ethanol injection, and percutaneous acetic acid injection to treat hepatocellular carcinoma of 3 cm or less. *Gut* 2005; **54**: 1151–6.
10 Llovet JM, Vilana R, Bru C *et al.* Increased risk of tumor seeding after percutaneous radiofrequency ablation for single hepatocellular carcinoma. *Hepatology* 2001; **33**: 1124–9.
11 Kim SH, Lim HK, Choi D *et al.* Percutaneous radiofrequency ablation of hepatocellular carcinoma: effect of histologic grade on therapeutic results. *AJR Am J Roentogenol* 2006; **186**: S327–33.
12 Takayasu K, Arii S, Ikai I *et al.* Prospective cohort study of transarterial chemoembolization for unresectable hepatocellular carcinoma in 8510 patients. *Gastroenterology* 2006; **131**: 461–9.
13 Ekelund L, Lin G, Jeppsson B. Blood supply of experimental liver tumors after intraarterial embolization with Gelfoam powder and absolute ethanol. *Cardiovasc Intervent Radiol* 1984; **7**: 234–9.
14 Kuroda C, Sakurai M, Monden M *et al.* Limitation of transcatheter arterial chemoembolization using iodized oil for small hepatocellular carcinoma. A study in resected cases. *Cancer* 1991; **67**: 81–6.

15 Hayashi M, Matsui O, Ueda K *et al.* Correlation between the blood supply and grade of malignancy of hepatocellular nodules associated with liver cirrhosis: evaluation by CT during intraarterial injection of contrast medium. *AJR Am J Roentogenol* 1999; **172**: 969–76.
16 Miyayama S, Matsui O, Yamashiro M *et al.* Iodized oil accumulation in the hypovascular tumor portion of early-stage hepatocellular carcinoma after ultraselective transcatheter arterial embolization. *Hepatol Int* 2007; **1**: 451–9.
17 Nakamura H, Hashimoto T, Oi H, Sawada S. Iodized oil in the portal vein after arterial embolization. *Radiology* 1998; **167**: 415–7.
18 Yuki K, Hirohashi S, Sakamoto M, Kanai T, Shimosato Y. Growth and spread of hepatocellular carcinoma: a review of 240 consecutive autopsy cases. *Cancer* 1990; **66**: 2174–9.
19 Terayama N, Matsui O, Gabata T *et al.* Accumulation of iodized oil within the non-neoplastic liver adjacent to hepatocellular carcinoma via the drainage routes of the tumor after transcatheter arterial embolization. *Cardiovasc Intervent Radiol* 2001; **24**: 383–7.
20 Hirota S, Nakao N, Yamamoto S *et al.* Cone-beam CT with flat-panel-detector digital angiography system: early experience in abdominal interventional procedures. *Cardiovasc Intervent Radiol* 2006; **29**: 1034–8.

Abdominal Imaging

Published online: 29 March 2008

Abdom Imaging (2009) 34:502–506
DOI: 10.1007/s00261-007-9254-9

Detection of hepatocellular carcinoma by CT during arterial portography using a cone-beam CT technology: comparison with conventional CTAP

Shiro Miyayama,[1] Osamu Matsui,[2] Masashi Yamashiro,[1] Yasuji Ryu,[1] Harumi Takata,[1] Taro Takeda,[1] Hiroyuki Aburano,[1] Noriaki Shigenari[1]

[1]Diagnostic Radiology, Fukuiken Saiseikai Hospital, 7-1, Funabashi, Wadanaka-cho, Fukui, Japan
[2]Radiology, Kanazawa University, Graduate School of Medical Science, Kanazawa, Japan

Abstract

Background: To evaluate the detectability of hepatocellular carcinoma (HCC) by computed tomography during arterial portography (CTAP) using cone-beam CT technology (CBCTAP) by comparing it with conventional CTAP.

Methods: Forty-four HCC lesions (mean diameter 1.9 ± 1.1 cm) of 24 patients who sequentially underwent conventional CTAP and CBCTAP during the same angiography session were evaluated. CBCTAP findings of each tumor were classed into three grades as compared to conventional CTAP: optimal; suboptimal; and nondiagnostic.

Results: All CBCTAP images had image artifacts from the catheter placed in the superior mesenteric artery and enhanced portal veins. Additionally, the contrast between HCC lesion and surrounding liver parenchyma of CBCTAP images was less than that of CTAP images. Of the 44 tumors, findings of 31 nodules (mean 2.2 ± 1.2 cm) (70.5%) were classed as optimal. Eight nodules (mean 1.4 ± 0.8 cm) (18.2%) were classed as suboptimal. Five nodules (mean 1.0 ± 0.1 cm) (11.4%) including two located in the outside of field of view were classed as nondiagnostic.

Conclusion: CBCTAP had sufficient image quality to detect almost all small HCC lesions compared to conventional CTAP and could depict approximately 89% of HCC nodules, including eight suboptimal lesions.

Correspondence to: Shiro Miyayama; *email:* +81-776-231111+81-776-288519miyayama@fukui.saiseikai.or.jp

Key words: Hepatocellular carcinoma—CT during arterial portography—Cone-beam CT technology—Angiography—Detectability

Introduction

Computed tomography (CT) during arterial portography (CTAP) is the most sensitive modality to detect hepatocellular carcinoma (HCC) [1, 2]. However, performing CTAP is slightly complicated because it is necessary to transfer the patient from the angiography room to the CT room. A combined CT-angiography system can resolve this problem, but it is relatively expensive [3].

Cone-beam CT (CBCT) technology using a flat-panel detector (FPD) is an alternative method of obtaining CT-like images without transferring or moving the patient [4, 5]. We used this technique to obtain CTAP images in patients with HCC. To evaluate the image quality of CBCTAP, we sequentially performed both CTAP images using a CT scanner (conventional CTAP) and CBCT technology (CBCTAP) during transcatheter arterial chemoembolization (TACE) for HCC. This study retrospectively evaluated the detectability of HCC nodules by CBCTAP compared to that by conventional CTAP.

Materials and methods

Patients

Between May 2006 and July 2006, CBCTAP was performed in 62 patients with HCC during the TACE

procedure. Before performing CBCTAP, the patient tried to hold the breath for 20 s and only patients who could complete the breath-holding test underwent CBCTAP. Written informed consent was obtained from each patient before the procedure. Institutional review board approval for this type of retrospective study was not required at our institution. We selected 24 patients in the present study. The patient selection criteria were as follows: (1) patients who had fewer than four nodular HCC lesions (2) patients who sequentially underwent conventional CTAP and CBCTAP.

Twenty-four patients met our criteria. There were 18 men and 6 women with a mean patient age of 69.0 ± 6.0 years (range 56–80 years). All patients had chronic hepatitis or liver cirrhosis. This was related to hepatitis C in 20 patients and hepatitis B in two patients. The etiology was unknown in two patients. The diagnosis of HCC was based on nodular staining on dynamic CT, dynamic MR imaging, angiography or CT during hepatic arteriography (CTHA), and nodular perfusion defect on conventional CTAP in addition to elevation of tumor markers. Six lesions were local progressive tumors after TACE. In total, 44 tumors with a mean diameter 1.9 ± 1.1 cm (range 0.7–5.5 cm) were demonstrated on conventional CTAP.

Technique of conventional CTAP

Conventional CTAP was performed before CBCTAP in all patients followed by arteriograms of celiac and superior mesenteric artery. After a 4-F catheter was inserted into the superior mesenteric artery in the angiography room, the patients were transferred to the CT room. Seventy milliliter of diluted contrast material [35 mL of 370 mgI iopamidol (Iopamiron 370; Schering, Osaka, Japan) or 350 mgI iomeprol (Iomeron 350; Ezai, Tokyo, Japan) and 35 mL of saline] was injected through the catheter at a rate of 3 mL/s after administration of 2.5 μg of prostaglandin E1 (Liple; Mitsubishi Pharma Corporation, Osaka, Japan). All patients were scanned with a multidetector-row helical CT scanner [Aquilion-16 (n = 8) or Aquilion-64 (n = 16); Toshiba, Tokyo, Japan] 35 s after the beginning of the injection of contrast material with 1- or 2-mm collimation, 3-mm thick sections and 3-mm-reconstruction intervals under a single breath hold.

Technique of CBCTAP

The patient was sent back to the angiography room after performing conventional CTAP. An angiographic unit with a 38 × 30 cm FPD (Allula Xper FD20, Philips Medical Systems, Best, The Netherlands) was used in all patients to obtain CBCTAP. A prototype of the CBCT software (XperCT; Philips Medical systems) was made available by the manufacturer. Six hundred twenty-one projection images were obtained by 20-s acquisition with 207° rotation of the FPD of the angiographic C-arm around the patient. Forty milliliter of non-diluted 370 mgI iopamidol or 350 mgI iomeprol was injected at a rate of 3 mL/s through the catheter after administration of 2.5 μg of prostaglandin E1. Scan began 20 s after the beginning of the injection of contrast material. Oxygen was administered to patients to minimize discomfort during breath holding. CT-like images were obtained 3 min after scanning at optional cross-section using a workstation (Philips Medical Systems). The axial images were reconstructed with 3-mm-intervals and compared to conventional CTAP images.

Image analysis

In the present study, we defined the gold standard for diagnosis of HCC as conventional CTAP findings. CBCTAP findings of each tumor were classified into three grades compared to conventional CTAP: (1) optimal, the tumor was clearly detectable as well as conventional CTAP; (2) suboptimal, the tumor was faintly detectable compared to conventional CTAP; and (3) nondiagnostic, the tumor could not be detected. Two experienced radiologists retrospectively evaluated all CTAP and CBCTAP images by consensus.

Results

All CBCTAP images had image artifacts from the catheter placed in the superior mesenteric artery and enhanced portal veins (Fig. 1). Additionally, the contrast between HCC lesion and surrounding liver parenchyma of CBCTAP images was less than that of CTAP images (Figs. 1, 2, 3, 4, 5).

Of the 44 tumors, 31 nodules (mean 2.2 ± 1.2 cm ; range 0.8–5.5 cm) (70.5%) were classed as optimal (Fig. 2). Eight nodules (mean 1.4 ± 0.8 cm; range 0.7–3.3 cm) (18.2%) were classed as suboptimal. In two recurrent tumors after TACE (3.3 and 1.2 cm in diameter, respectively), arterioportal shunt near the tumor caused the findings to become unclear. In other two nodules (both 1.5 cm in diameter) intratumoral portal blood was slightly preserved, there was little contrast between the tumor and liver parenchyma compared to that on conventional CTAP findings (Fig. 3). One tumor, 1.8 cm in diameter became unclear because of artifact from the densely accumulated iodized oil. The remaining three nodules measured less than 1 cm in diameter. Five nodules (mean 1.0 ± 0.1 cm ; range 0.9–1 cm) (11.4%) were classed as nondiagnostic. Two tumors, 1 cm in diameter in one patient could not be detected because of artifacts from the iodized oil and portal veins, in addition to inadequate enhancement of the liver parenchyma. Two nodules (both 1 cm in diameter) in

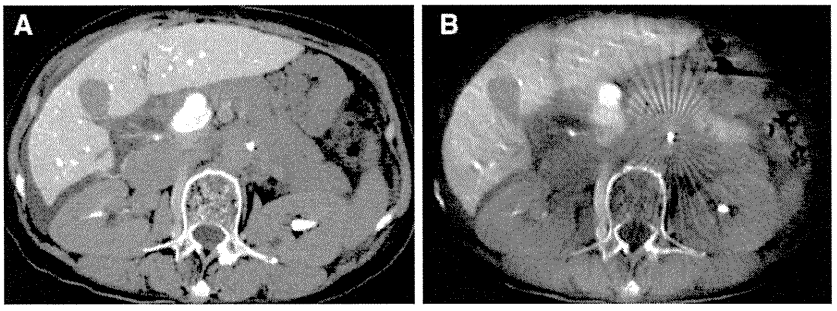

Fig. 1. A 71-year-old woman with HCC. **A** Conventional CTAP image shows a hypoattenuating mass in the right lobe of the liver. **B** CBCTAP image clearly shows the hypoattenuating mass. However, strong image artifacts from a catheter placed in the superior mesenteric artery are also seen.

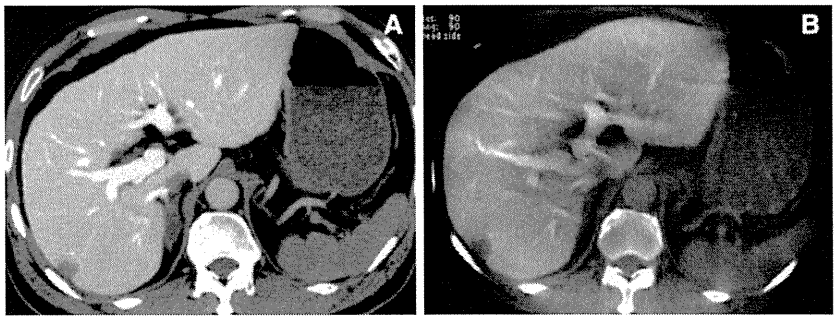

Fig. 2. A 59-year-old man with HCC. **A** Conventional CTAP image shows a hypoattenuating mass in the right lobe of the liver. **B** CBCTAP image clearly shows the tumor along with a small artifact from the portal branches.

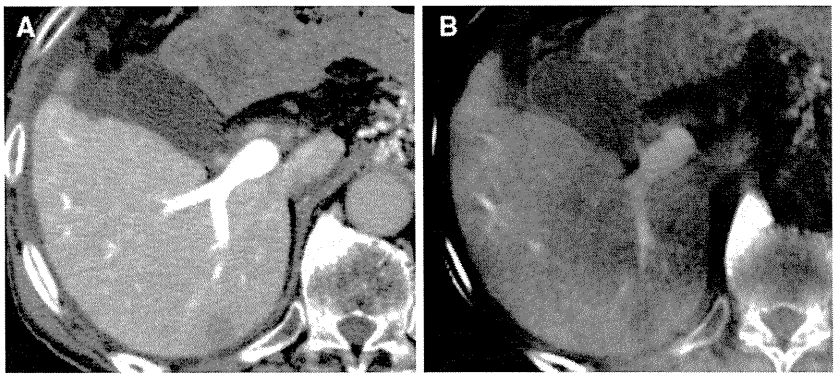

Fig. 3. A 71-year-old man with HCC partially supplied by the portal blood. **A** Conventional CTAP image shows a slightly hypoattenuating mass in the right lobe of the liver. **B** CBCTAP image shows a faint hypoattenuating mass. The contrast between the tumor and surrounding liver parenchyma is low compared to that at conventional CTAP.

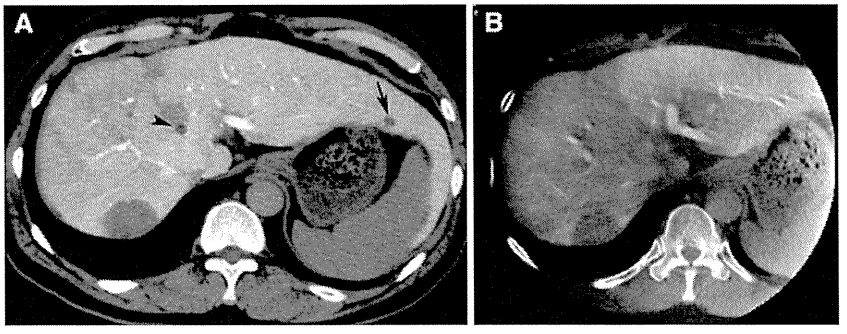

Fig. 4. A 56-year-old man with multiple HCC. **A** Conventional CTAP image shows a large tumor in the right lobe of the liver and small tumor in the left lobe of the liver (*arrow*). A small cyst is also seen in the left lobe of the liver (*arrowhead*). **B** CBCTAP image depicts the large tumor, but the small tumor is outside of FOV. The small cyst in the left lobe of the liver was depicted in another image (not shown).

one patient located in the lateral segment of the liver did not include the field of view (FOV) of CBCTAP images. The remaining nodule was less than 1 cm in diameter (Fig. 4).

CBCTAP did not detect any nodular lesions suspected of being HCC other than those already shown at conventional CTAP findings.

Discussion

CTAP is the most reliable imaging modality for the diagnosis of malignant hepatic lesions [1, 2]. CTAP provides the radiologist with useful information concerning not only the number of HCC lesions but also the malignancy grades of hepatocyte nodules originating in

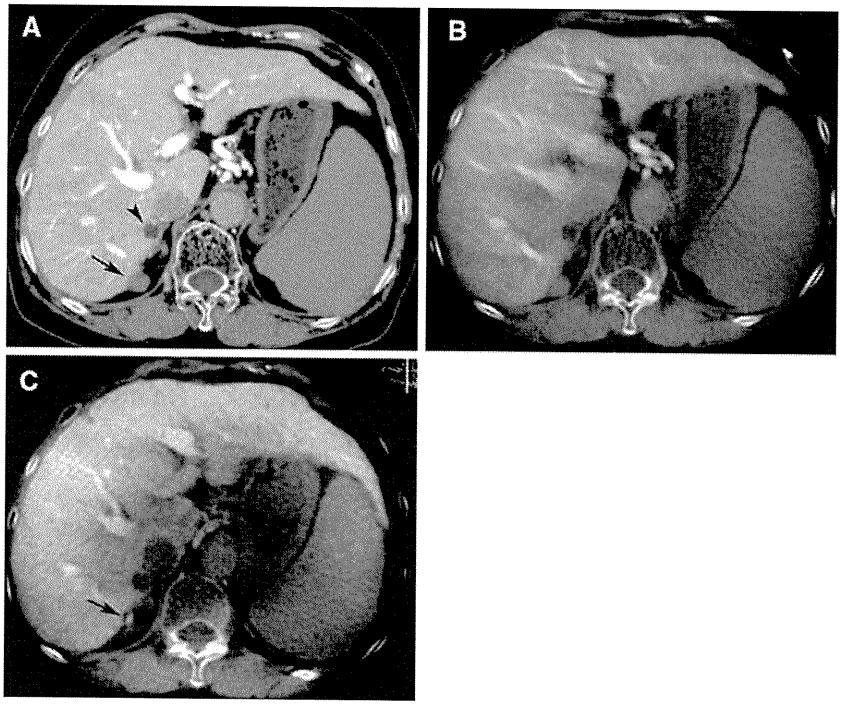

Fig. 5. A 68-year-old woman with HCC in the right lobe of the liver. **A** Conventional CTAP image shows a tumor (*arrow*) and cyst (*arrowhead*) in the right lobe of the liver. **B** CBCTAP image obtained using a prototype of XperCT software shows both lesions, but artifacts from the portal branches are also seen. **C** CBCTAP image obtained five months later using commercially available XperCT software shows that artifacts from the portal branches are improved although the image becomes slightly coarse. The size of the tumor also shrinks due to the effect of previous TACE (*arrow*).

the cirrhotic liver [2]. We have routinely performed CTAP immediately before TACE for HCC, although transferring patients to the CT room prolongs the procedure. Although a combined CT-angiography system is now commercially available [3], it is expensive and requires a large room. In addition, the movement of the patient, C-arm, or CT gantry is needed to obtain CT images. However, CBCTAP can be obtained simply by lifting the patients' hands without other movement.

CBCT is a new technology to obtain CT-like images using a C-arm system while rotating it around the patient [4–7]. A C-arm system equipped with a large FPD could obtain a high image quality and large FOV compared to that obtained by the image-intensified system. This technology has been introduced in the interventional procedures [4, 5]; however, there are no reports concerning the detectability of CBCT for liver tumors. In the present study, we evaluated the detectability of CBCTAP for HCC lesions compared to conventional CTAP.

CBCTAP could depict approximately 89% of HCC nodules in the present study, including eight suboptimal lesions. We think that CBCTAP has sufficient image quality to detect almost all small HCC lesions. Smaller lesions or lesions partially supplied by portal blood tended to be suboptimal at CBCTAP images. Artifacts from the catheter, portal branches, or densely accumulated iodized oil may also make it difficult to detect small lesions. Advanced algorithm, to reduce these image artifacts, may be needed to improve the image quality. Motion artifacts mainly caused by inadequate breath holding may also deteriorate the image quality; therefore, a faster scanning protocol may be necessary. In addition, FOV of CBCTAP seems too small to observe the entire liver. In the present study, two HCC lesions located in the lateral segment of the liver did not include FOV of CBCTAP. Decreasing source-to-image receptor distance during scanning may resolve this problem.

There are several limitations in the present study. First, the gold standard for diagnosis of HCC in this study was conventional CTAP findings. This means that HCC nodules that were not detected by conventional CTAP images are not evaluated. However, there are many reports describing the excellent image quality of CTAP for detecting HCC lesions [1, 2]. We consider that CTAP has sufficient capacity to depict HCC lesions that require treatment. Second, angiography and conventional CTAP were performed before CBCTAP in all cases. This may reduce the contrast between HCC lesions and surrounding liver parenchyma on CBCTAP images because of the retention of previously injected contrast material in the tumor interstitium. However, several minutes were needed to return to the angiography room after CTAP and contrast material might be washed out from the tumor until the start of CBCTAP. Third, we excluded patients who could not hold their breath for 20 s. This might have caused a bias in patient selection because the scanning time was too long for elderly patients.

CBCT technology has several advantages over conventional CT technology. The image data are obtained as isotropic voxel data with superior spatial resolution. Slice thickness and image direction can be adjusted as desired. Simultaneously, 3D-angiography images with the maximum intensity projection (MIP) technique can also be obtained. In addition, CBCT technology can

reduce the irradiation dose compared to conventional CT [5]. CBCTAP is a new modality with great potential, although the total amount of contrast material, injection rate, and delayed time to start scanning require further investigation to obtain better images.

In conclusion, CBCTAP has sufficient image quality to detect almost all of the small HCC lesions that can be detected by conventional CTAP, although the images have several noises. This new imaging technology may reduce the stress both on the patient and radiologist during the TACE procedure and may provide useful information.

Appendix

Since September 2006, we have used a commercially available XperCT software (Philips Medical Systems) with 10-s acquisition. The total amount of contrast material and injection rate were not changed, but the scanning delay time of CBCTAP was changed to 25 s. The reconstruction time was reduced to 90 s. The image artifacts were improved by the new acquisition technique, although the image became slightly coarser because half of image projections were acquired during the scanning compared to the prototype technique (Fig. 5). Almost all TACE procedures could be performed in the angiographic room without transferring the patient to the CT room.

References

1. Matsui O, Kadoya M, Suzuki M, et al. (1983) Work in progress: dynamic sequential computed tomography during arterial portography in the detection of hepatic neoplasms. Radiology 146:721–727
2. Matsui O, Kadoya M, kameyama T, et al. (1991) Benign and malignant nodules in cirrhotic livers: distinction based on blood supply. Radiology 178:493–497
3. Ishijima H, Koyama Y, Aoki J, et al. (1999) Use of a combined CT-angiography system for demonstration of correlative anatomy during embolotherapy for hepatocellular carcinoma. J Vasc Interv Radiol 10:811–815
4. Binkert CA, Alencar H, Singh J, et al. (2006) Translumbar type II endoleak repair using angiographic CT. J Vasc Interv Radiol 17:1349–1353
5. Hirota S, Nakao N, Yamamoto S, et al. (2006) Cone-beam CT with flat-panel-detector digital angiography system: early experience in abdominal interventional procedures. Cardiovasc Intervent Radiol 29:1034–1038
6. El-Sheik M, Heverhagen JT, Alfke H, et al. (2001) Multiplanar reconstructions and three-dimensional imaging (computed rotational osteography) of complex fractures by using a C-arm system: initial results. Radiology 221:843–849
7. Linsenmaier U, Rock C, Euler E, et al. (2002) Three-dimensional CT with a modified C-arm image intensifier: feasibility. Radiology 224:286–292

Cardiovasc Intervent Radiol (2009) 32:255–264
DOI 10.1007/s00270-008-9468-4

CLINICAL INVESTIGATION

Usefulness of Cone-Beam Computed Tomography During Ultraselective Transcatheter Arterial Chemoembolization for Small Hepatocellular Carcinomas that Cannot be Demonstrated on Angiography

Shiro Miyayama · Masashi Yamashiro · Miho Okuda · Yuichi Yoshie · Natsuki Sugimori · Saya Igarashi · Yoshiko Nakashima · Osamu Matsui

Received: 14 April 2008 / Accepted: 30 October 2008 / Published online: 9 December 2008

Abstract This study evaluated the usefulness of cone-beam computed tomography (CBCT) during ultraselective transcatheter arterial chemoembolization (TACE) for hepatocellular carcinomas (HCC) that could not be demonstrated on angiography. Twenty-eight patients with 33 angiographically occult tumors (mean diameter 1.3 ± 0.3 cm) were enrolled in the study. The ability of CBCT during arterial portography (CBCTAP), during hepatic arteriography (CBCTHA), and after iodized oil injection (LipCBCT) to detect HCC lesions was retrospectively analyzed. The technical success of TACE was divided into three grades: complete (the embolized area included the entire tumor with at least a 5-mm wide margin), adequate (the embolized area included the entire tumor but without a 5-mm wide margin in parts), and incomplete (the embolized area did not include the entire tumor) according to computed axial tomographic (CAT) images obtained 1 week after TACE. Local tumor progression was also evaluated. CBCTAP, CBCTHA, and LipCBCT detected HCC lesions in 93.9% (31 of 33), 96.7% (29 of 30), and 100% (29 of 29) of patients, respectively. A single branch was embolized in 28 tumors, and 2 branches were embolized in five tumors. Twenty-seven tumors (81.8%) were classed as complete, and 6 (18.2%) were classed as adequate. None of the tumors were classed as incomplete. Twenty-five tumors (75.8%) had not recurred during 12.0 ± 6.2 months. Eight tumors (24.2%), 5 (18.5%) of 27 complete success and 3 (50%) of 6 adequate success, recurred during 10.1 ± 6.2 months. CBCT during TACE is useful in detecting and treating small HCC lesions that cannot not be demonstrated on angiography.

Keywords Cone-beam computed tomography · Hepatocellular carcinoma · Transcatheter arterial chemoembolization

S. Miyayama (✉) · M. Yamashiro · M. Okuda · Y. Yoshie · N. Sugimori · S. Igarashi · Y. Nakashima
Department of Diagnostic Radiology, Fukuiken Saiseikai Hospital, 7-1 Funabashi, Wadanaka-cho, Fukui 918-8503, Japan
e-mail: s-miyayama@fukui.saiseikai.or.jp

O. Matsui
Department of Radiology, Kanazawa University Graduate School of Medical Science, 13-1, Takara-machi, Kanazawa 920-8641, Japan

Introduction

Hepatocellular carinoma (HCC) is the fifth most common cancer worldwide. Although it has become possible to diagnose small HCC lesions with advancement in imaging technology and establishment of a high-risk group, the prognosis remains poor because of the associated hepatic impairment and high intrahepatic recurrence rate [1].

Transcatheter arterial chemoembolization (TACE) is one of the effective therapeutic options for inoperable HCC lesions [1–5]. We have performed ultraselective TACE to improve local control and to decrease adverse effects [5]. However, angiography frequently cannot demonstrate small HCC lesions because of decreased hypervascularity, and TACE is reluctantly performed to a relatively large area because of difficulty in identifying the feeding vessel. Recently, cone-beam computed tomographic (CBCT) technology using a flat-panel detector (FPD) has become available [6–10], and we used this technique in combination with ultraselective TACE for HCC lesions. In this study, we analyzed the ability of several CBCT techniques to detect HCC lesions with a mean diameter of 1.3 cm as well as report the technical success rates of ultraselective

TACE assisted by CBCT for HCC lesions that could not be demonstrated on angiography.

Materials and Methods

This was a retrospective study to evaluate the usefulness of CBCT during TACE procedure for small HCC lesions that could not be demonstrated on angiography. Institutional Review Board approval is not required at our institution for this type of retrospective study. Written informed consent was obtained from each patient before undergoing TACE.

Patients

Between September 2006 and March 2008, 532 TACE procedures were performed in our hospital in 299 patients with inoperable HCC lesions. Among them, we reviewed 33 angiographically occult HCC lesions of 28 patients treated with TACE assisted by CBCT technology. All tumors were diagnosed as HCC lesions based on imaging findings. The diagnosis of all HCC lesions was established by (1) a combination of nodular enhancement on arterial phase and wash of contrast material on delayed phase on double arterial-phase dynamic computed axial tomography (CAT) obtained using a multidetector-row helical CAT scanner (MDCAT; Aquilion-16 or Aquilion-64; Toshiba, Tokyo, Japan) and (2) presence of a nodular perfusion defect on CAT during arterial portography (CTAP and/or CBCTAP). In dynamic CAT, the first arterial-phase images were obtained 35 s after the start of injection of 100 ml 300 mg I/ml iohexol (Omunipaque 300; Daiichi-Sankyo, Tokyo, Japan) at a rate of 3 ml/s, and the second arterial-phase images were obtained 45 s after injection of contrast material. These two arterial-phase images were accomplished in a single breath hold. Delayed-phase images were obtained 180 s after injection of contrast material. The tumor selection criteria were as follows: (1) a tumor that did not show an obvious tumor stain on angiography and (2) a tumor that had not been previously treated, including a newly developed tumor during follow-up after HCC treatment. Thirty-three HCC lesions in 28 patients met these criteria. There were 19 men and 9 women (mean age [± SD] 71.3 ± 6.9 years [range 57 to 84]). All patients had chronic hepatitis or liver cirrhosis. This was related to hepatitis C in 19 patients, to hepatitis B in 1 patient, and to habitual alcohol complication in 2 patients. The etiology was unknown in 6 patients. Three patients had 2 tumors, including 1 patient who had 2 tumors develop asynchronously. One patient had 3 tumors. In total, these patients had 33 tumors that could not be detected on angiography (mean diameter 1.3 ± 0.3 cm [range 0.8 to 2.4 cm, median 1.2 cm]) (Table 1). Twenty-one tumors were initially demonstrated, and 12 were newly developed during follow-up after HCC treatment. Five patients also had another tumor that showed an obvious tumor stain on angiography. Serum levels of α-fetoprotein were >21 μg/l in 8 patients (21 to 100 μg/l [$n = 4$], 101 to 400 μg/l [$n = 3$], and >401 μg/l [$n = 1$]). Serum levels of protein induced in vitamin K absence II (PIVKA-II) were >41 mAU/ml (μg/l) in 11 patients (41 to 100 mAU/ml [$n = 8$], 101 to 400 mAU/ml [$n = 2$], and >401 mAU/ml [$n = 1$]). In 2 patients, serum levels of both tumor markers were elevated. In 11 patients (39.2%), serum levels of both tumor markers were normal. None of the tumors were candidates for surgical resection because of poor hepatic function reserve or patient refusal. None of the tumors were also candidates for radiofrequency (RF) ablation because of the difficulty in detecting the tumor on sonography and unenhanced CAT, presence of ascites, tumor location near vulnerable structures, or patient refusal to undergo RF ablation.

CBCT Technique

An angiographic unit with a 38 × 30 cm FPD (Allula Xper FD20; Philips Medical Systems, Best, The Netherlands) was used to obtain CBCT images. Three-hundred twelve projection images with X-ray parameters of 120 kV and 200 to 300 mAs were obtained by 10-s acquisition with 207° rotation around the patient of the FPD of the angiographic C-arm. Oxygen was administered to patients during the procedure to minimize the discomfort of breath holding.

Three different CBCT techniques (XperCT; Philips Medical Systems) were used:

1. CBCTAP was routinely performed at the beginning of the procedure. Forty ml contrast material (370 mg I/ml iopamidol [Iopamiron 370; Bayer, Osaka, Japan] or 350 mg I/ml iomeprol [Iomeron 350; Ezai, Tokyo, Japan] was injected at a rate of 3 ml/s through a 4F catheter placed into the superior mesenteric artery after administration of 2.5 μg prostaglandin E1 (Liple; Mitsubishi Pharma Corporation, Osaka, Japan). When the replaced hepatic branches or the arterial flow toward the liver from the superior mesenteric artery was demonstrated, the catheter tip was deeply advanced beyond these branches. The scan began 25 s after the beginning of the injection of contrast material.
2. CBCTHA was performed at the common or proper hepatic, right or left hepatic, or selected small branch of the liver. When CBCTHA was performed at the common or proper hepatic artery, 25 ml half-diluted contrast material was injected at a rate of 1.5 ml/s through a 4F catheter. When CBCTHA was performed

Table 1 Summary of 33 tumors of 28 patients

Patient no./age (y)/sex	Tumor diameter (cm)	Segment	CBCTAP	CBCTHA	LipCBCT	No. of embolized branches	Grades of technical success	Outcomes (mo)
1/76/M	1.8	S6	Depicted	–	Depicted	1	Complete	Controlled (25)
	2.4	S5	Depicted	Depicted	Depicted	2	Complete	Controlled (14)
2/69/F	0.8	S8	Depicted	Depicted	Depicted	1	Complete	Recurred (20)
3/57/M	1	S8	Not depicted	Not depicted	Depicted	1	Complete	Controlled (24)
4/59/M	1.3	S7	Depicted	Depicted	–	1	Complete	Controlled (20)
5/69/M	1.6	S3	Depicted	Depicted	Depicted	1	Complete	Controlled (15)
6/61/M	1.2	S7	Depicted	Depicted	Depicted	1	Complete	Recurred (2)
7/65/M	1.1	S2	Depicted	–	Depicted	1	Complete	Controlled (20)
8/75/M	1.5	S6	Depicted	Depicted	Depicted	1	Complete	Recurred (15)
9/69/M	1.6	S4	Depicted	–	Depicted	1	Complete	Controlled (19)
10/75/M	1	S4	Depicted	Depicted	Depicted	1	Complete	Controlled (15)[a]
11/71/M	1.1	S8/7	Depicted	Depicted	Depicted	2	Complete	Controlled (16)
12/65/M	1	S2	Depicted	Depicted	Depicted	1	Complete	Controlled (15)
13/84/F	1.2	S8	Depicted	Depicted	–	1	Complete	Controlled (16)
14/70/F	1.4	S6	Depicted	Depicted	Depicted	2	Complete	Recurred (12)
15/74/M	1.3	S6	Depicted	Depicted	Depicted	1	Adequate	Recurred (10)
16/69/M	1.3	S8	Depicted	Depicted	–	1	Adequate	Recurred (9)
17/67/M	1.7	S3	Depicted	Depicted	Depicted	1	Complete	Controlled (6)[b]
18/65/M	1	S6	Not depicted	Depicted	Depicted	1	Complete	Controlled (11)
19/74/F	1.4	S7	Depicted	Depicted	Depicted	1	Adequate	Controlled (12)
20/75/F	1.2	S1	Depicted	Depicted	Depicted	1	Complete	Recurred (2)
21/83/F	1	S1	Depicted	Depicted	Depicted	1	Adequate	Recurred (11)
22/74/M	1	S6	Depicted	Depicted	Depicted	1	Complete	Controlled (10)
23/73/F	1.7	S2	Depicted	Depicted	Depicted	1	Complete	Controlled (8)
24/66/F	1	S1	Depicted	Depicted	Depicted	1	Adequate	Controlled (8)
	1.7	S5/6	Depicted	Depicted	Depicted	2	Complete	Controlled (8)
25/80/M	1.5	S8	Depicted	Depicted	Depicted	1	Complete	Controlled (4)
	1	S8	Depicted	Depicted	Depicted	1	Adequate	Controlled (4)
	0.8	S6	Depicted	Depicted	–	1	Complete	Controlled (4)
26/72/M	1	S7/6	Depicted	Depicted	Depicted	2	Complete	Controlled (7)
27/83/M	1.2	S8	Depicted	Depicted	Depicted	1	Complete	Controlled (7)
	1	S8	Depicted	Depicted	Depicted	1	Complete	Controlled (7)
28/77/F	1.2	S6	Depicted	Depicted	Depicted	1	Complete	Controlled (7)

[a] The patient died 16 months after TACE from rapid tumor progression at other sites

[b] The patient suddenly died from arrhythmia 8 months after TACE

at a more distal level of the right or left hepatic artery, 5 ml half-diluted contrast material was slowly injected manually through a 2F tip microcatheter (Progreat α; Terumo, Tokyo, Japan). The scan began 7 s after the beginning of the injection of contrast material.

3. CBCT was also performed after injection of a mixture of iodized oil (Lipiodol; Andre Guerbet, Aulnaysous-Bois, France) and anticancer drugs (LipCBCT). A mixture of 1 to 3 ml iodized oil (almost equal to the diameter of the tumor, e.g., a 2-cm tumor with 2 ml iodized oil), 10 to 20 mg epirubicin (Farmorbicin; Kyowa Hakko, Tokyo, Japan), and 2 to 4 mg mitomycin C (Mitomycin; Kyowa Hakko) was prepared, and CBCT was performed after injection of approximately 1 to 2 ml of the mixture. This technique was mainly performed when blood supply to the tumor from the selected branch was highly suspected or when iodized oil accumulation in the tumor was unclear during TACE despite tumor feeding on selective CBCTHA images. In addition, this technique was

performed when the selected branch was too minute and contrast material easily overflowed despite careful hand injection. When multiple small branches were each sequentially embolized after performing selective CBCTHA, we also regarded additional CBCTHA at one small branch obtained after TACE of another small branch as LipCBCT.

All CAT-like images were obtained 90 s after scanning at optional cross-section using a workstation (Philips Medical Systems). Images, 3-mm thick, were used for observation. Conventional CTAP was performed using an MDCAT scanner (Aquilion-64; Toshiba) when CBCTAP could not depict the target tumor.

TACE Procedure

We defined ultraselective TACE as TACE at the most distal portion of the subsubsegmental artery of the liver. A 2F tip microcatheter was advanced into the target branch through a 4F catheter placed in the celiac, superior mesenteric, or common hepatic artery. To navigate the microcatheter, a 0.016-inch guidewire (GT-Wire; Terumo) was routinely used in all patients. When selection of the feeding branch by the 0.016-inch guidewire was difficult, a 0.012-inch guidewire (GT-Wire; Terumo) was used. The target branch was identified according to tumor location and findings on CBCTAP and CBCTHA images.

After the microcatheter was inserted into the target branch, selective CBCTHA or LipCBCT was performed to confirm whether the branch fed the tumor. When there was no apparent feeding to the target tumor, additional CBCT was performed after another branch was selected. When blood supply to the target tumor through the selected branch was identified, TACE was performed by injection of a mixture of iodized oil and anticancer drugs followed by gelatin sponge particles (Gelfoam; Upjohn, Kalamazoo, MI [until December 2006] or Gelpart; Nihon Kayaku, Tokyo, Japan [since January 2007]). When the entire tumor was not embedded in the vascular territory of the selected branch, another feeding vessel was selected and sequentially embolized in the same fashion. The TACE procedure was ended when the entire tumor was included in the embolized area on CBCT images. In five patients who had additional tumors showing tumor stain on angiography, the tumor was sequentially treated with ultraselective TACE.

Definition of Technical Success and Follow-Up Protocol

Unenhanced CAT was performed 1 week after TACE in all patients to check iodized oil distribution not only in the tumor but also in the surrounding liver parenchyma. We defined the embolized area where iodized oil was retained at 1 week after CAT. According to these CAT images, technical success was divided into three grades: complete, adequate, and incomplete: (1) complete was defined as the embolized area included the entire tumor with at least a 5-mm wide circumferential margin; (2) adequate was defined as the embolized area included the entire tumor but the 5-mm wide safety margin was not uniformly obtained along all parts of the circumference; and (3) incomplete was defined as the embolized area did not include the entire tumor.

Dynamic CAT every 2 to 3 months after TACE procedures was also performed in all patients to check local tumor recurrence. Magnetic resonance (MR) imaging was not routinely performed and was only performed in six patients when local recurrence could not be judged on CAT because of artifact from densely accumulated iodized oil in the tumor.

Results

Results for each tumor are listed in Table 1. CBCT was performed in 2 to 6 sessions (mean 3.8 ± 1.1) in each patient. CBCTAP was performed in all patients (100%). One to five sessions (mean 2.1 ± 1.1 sessions) of CBCTHA were performed in 30 tumors (90.9%) in 26 patients. CBCTHA at the common hepatic artery ($n = 10$), the proper hepatic artery ($n = 2$), or right hepatic artery ($n = 4$) was performed in 16 tumors in 13 patients, and selective CBCTHA at the distal portion of the subsubsegmental artery was performed in 26 tumors in 22 patients. LipCBCT was performed in 29 tumors (87.9%) in 25 patients. In 3 of these 25 patients, LipCBCT was performed twice. Both CBCTHA and LipCBCT were performed in 25 tumors in 22 patients. Either selective CBCTHA or LipCBCT was performed in all tumors. Conventional CTAP was performed in 2 tumors (6%) in 2 patients in whom the lesions could not be detected by CBCTAP.

Ability of Each CBCT Technique to Detect HCC Lesions

All but two tumors measuring 1 cm in diameter were detected on CBCTAP (Figs. 1 and 2). Conventional CTAP depicted the remaining two tumors. Therefore, detectability of HCC lesions on CBCTAP was 93.9%.

CBCTHA demonstrated 29 (96.7%) of 30 tumors (Figs. 1 through 3). The remaining tumor (1-cm diameter) that was not detected on CBCTAP was also undetectable on CBCTHA performed at the common hepatic artery. LipCBCT clearly depicted this lesion. Another tumor (1-cm diameter) that could not be detected on CBCTAP was detected on CBCTHA.

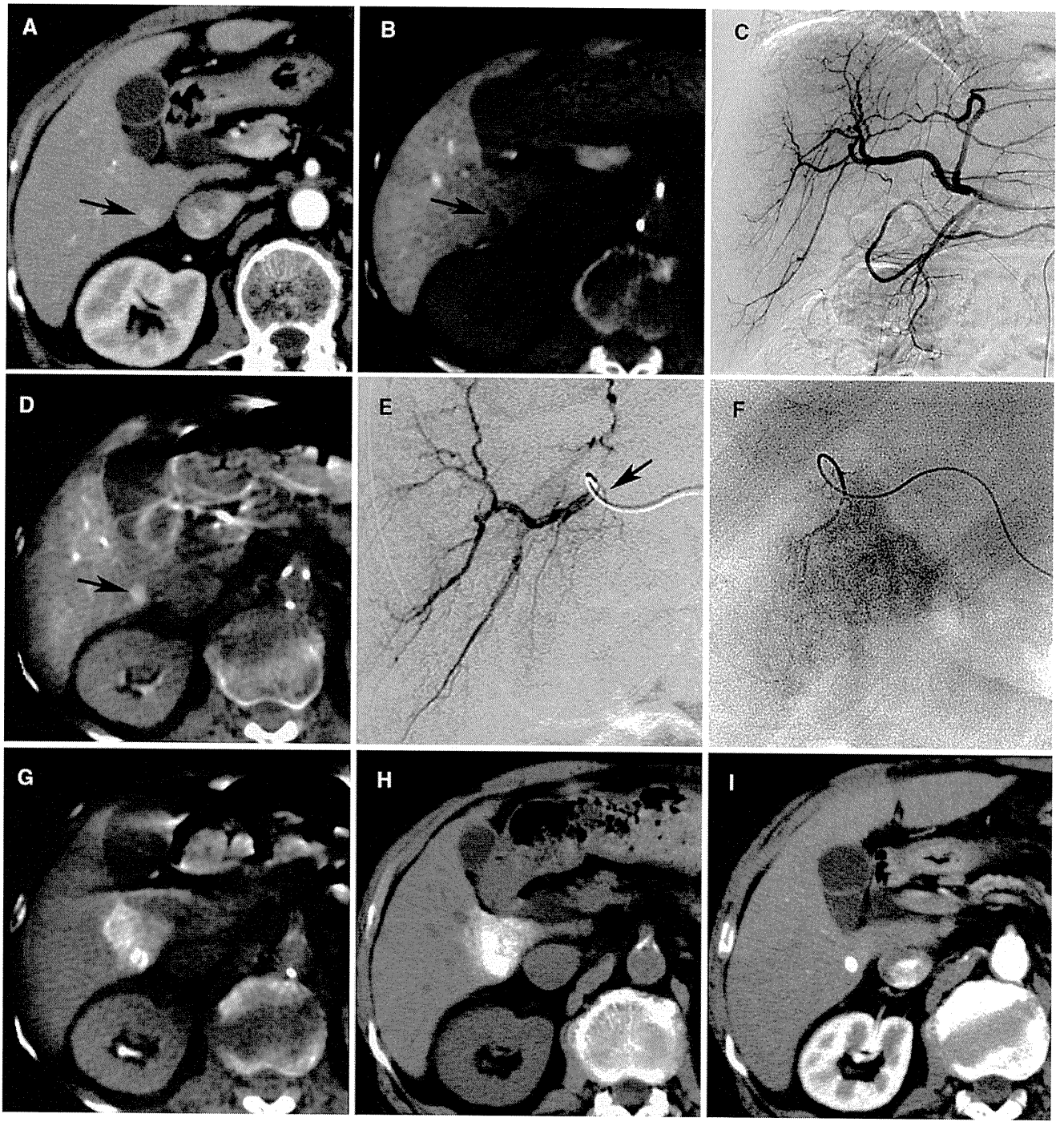

Fig. 1 A small HCC lesion in segment VI in a 76-year-old man. **A** Arterial-phase CAT shows a hyperatteunating tumor in segment VI (*arrow*). **B** CBCTAP shows a tumor as a nodular perfusion defect (*arrow*). **C** Arteriogram of the common hepatic artery does not show any obvious tumor stains. **D** CBCTHA at the common hepatic artery shows nodular enhancement (*arrow*). **E** Arteriogram of the posterior inferior subsegmental artery (A6) also does not show any tumor stains. The small branch derived from the proximate portion of A6 was suspected of being the tumor-feeding branch and was selected for embolization (*arrow*). **F** Spot radiograph obtained during iodized oil injection through the branch does not show obvious iodized oil accumulation in the tumor. **G** LipCBCT obtained after iodized oil injection clearly shows that the entire tumor is embedded in the territory of the embolized area. TACE was performed after additional injection of iodized oil. **H** CAT obtained 1 week after TACE shows dense iodized accumulation throughout the entire tumor, including a safety margin. **I** Arterial-phase CAT obtained 10 months after TACE shows dense iodized oil accumulation in the tumor without recurrence

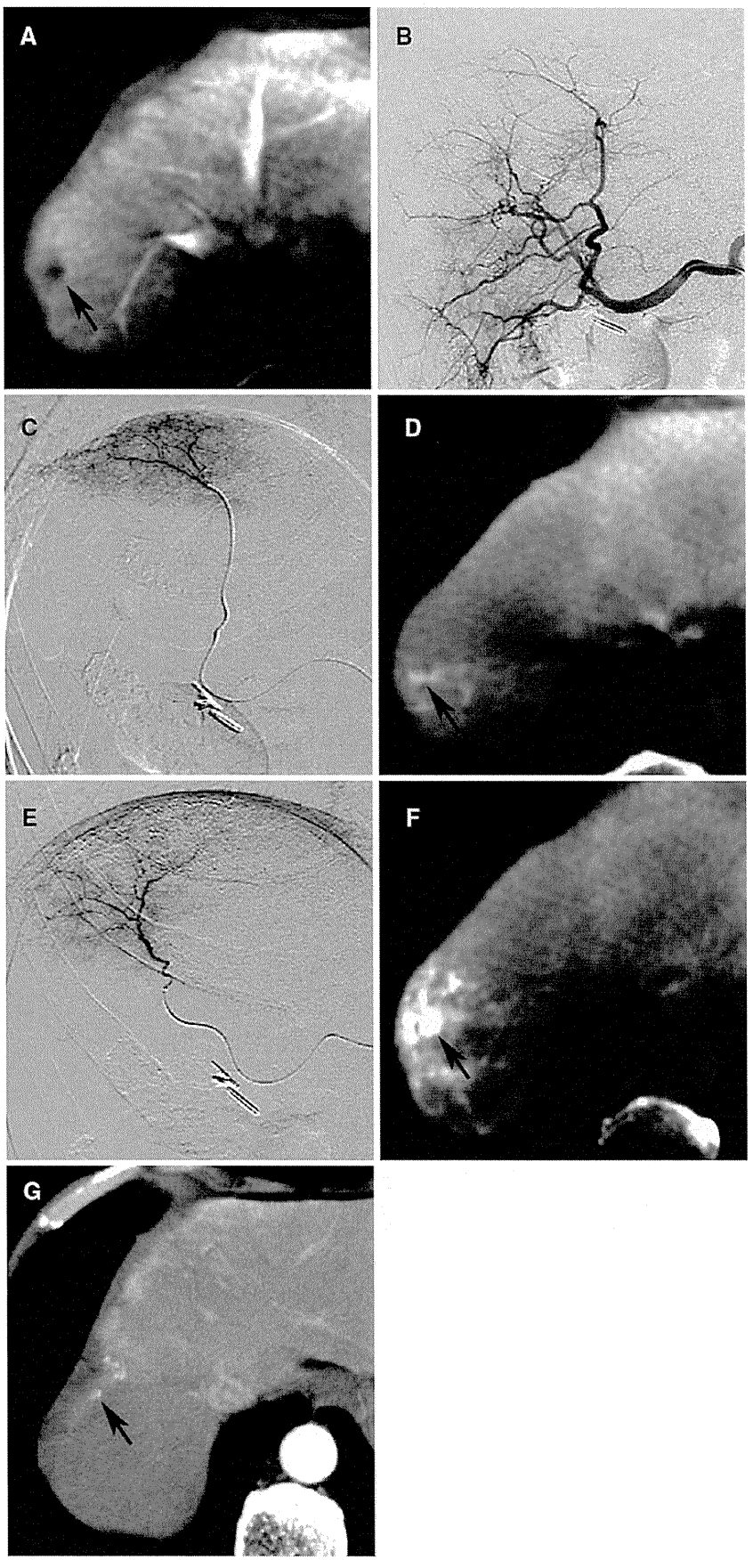

Fig. 2 A small HCC lesion at the boundary between segments VII and VIII in a 71-year-old man. **A** CBCTAP shows a nodular perfusion defect at the boundary between segments VII and VIII (*arrow*). **B** Arteriogram of the right hepatic artery does not show any obvious tumor stains. **C** Selective arteriogram of the branch of the posterior superior subsegmenal artery does not show any tumor stains. **D** Selective CBCTHA at the branch showed that the branch partially feeds the tumor (*arrow*). TACE of this branch was performed. **E** Selective arteriogram of the branch of the anterior superior subsegmental artery shows no tumor stains. Selective CBCTHA at the branch shows that this branch also feeds the tumor (not shown). TACE of the branch was started at this point. **F** LipCBCT at the branch shows dense iodized oil accumulation throughout the entire tumor (*arrow*). **G** Arterial-phase CAT obtained 14 months after TACE shows that the tumor has decreased in size without any evidence of local recurrence (*arrow*). Atrophy of the surrounding liver parenchyma is also seen